JPET Fast Forward. Published on December 17, 2012 as DOI: 10.1124/jpet.112.201475

JPET #201475

Title Page:

Mechanisms Limiting Distribution of the BRAF^{V600E} Inhibitor Dabrafenib to the Brain: Implications for the Treatment of Melanoma Brain Metastases

Rajendar K. Mittapalli, Shruthi Vaidhyanathan, Arkadiusz Z. Dudek, and William F. Elmquist

Department of Pharmaceutics, Brain-Barriers Research Center, University of Minnesota, Minneapolis, MN, USA (RKM, SV, WFE)

Divison of Hematology, Oncology and Transplantation, Department of Medicine, University of Minnesota. (AZD)

JPET Fast Forward. Published on December 17, 2012 as DOI: 10.1124/jpet.112.201475
This article has not been copyedited and formatted. The final version may differ from this version.

Running Title: Brain distribution of dabrafenib in mouse

Corresponding Author:

William F. Elmquist, Department of Pharmaceutics, University of Minnesota, 9-177 Weaver Densford Hall, 308 Harvard Street SE, Minneapolis, MN 55455, USA.

Phone: +001-612-625-0097; Fax: +001-612-626-2125; e-mail: elmqu011@umn.edu

Manuscript Statistics:

Number of Figures: **7**

Number of Tables: **5**

Number of Pages: **41**

Number of References: **40**

Number of words in Abstract: **251**

Number of words in Introduction: **804**

Number of words in Discussion: **1473**

Number of supplementary figures: **3**

List of abbreviations:

A to B, apical to basolateral; ABC, ATP-binding cassette; AUC, area under the curve; B to A, basolateral to apical; B/P, brain-to-plasma; BBB, blood-brain-barrier; BCRP, breast cancer resistance protein; *Bcrp1*, gene encoding the murine breast cancer resistance protein; BRAF, gene encoding serine/threonine-protein kinase B-Raf; CNS, central nervous system; DMSO, dimethyl sulphoxide; $f_{u,brain}$, unbound fraction in brain homogenate; $f_{u,plasma}$, Unbound fraction in plasma; FVB, Friend Leukemia Virus Strain B; Ko143, (3S,6S,12aS)-1,2,3,4,6,7,12,12a-octahydro-9-methoxy-6-(2-methylpropyl)-1,4-dioxopyrazino(1',2':1,6) pyrido(3,4-b)indole-3-propanoic acid 1,1-dimethylethyl ester; AG1478, 4-(3-Chloroanilino)-6,7-dimethoxyquinazoline; Kp = ratio of AUC_{brain} to AUC_{plasma}; LC-MS/MS, liquid chromatography-tandem mass spectrometry; LY335979 (zosuquidar), (R)-4-((1aR,6R,10bS)-1,2-difluoro-1,1a,6,10b-tetrahydrodibenzo-(a,e)cyclopropa(c)cycloheptan-6-yl)-α-((5-quinoloyloxy) methyl)-1-piperazine ethanol, trihydrochloride; MDCKII, Madin-Darby canine kidney II; MDR1, gene encoding the human p-glycoprotein; *Mdr1*, gene encoding the murine p-glycoprotein; P_{app}, apparent permeability; P-gp, p-glycoprotein;

JPET Fast Forward. Published on December 17, 2012 as DOI: 10.1124/jpet.112.201475
This article has not been copyedited and formatted. The final version may differ from this version.

Abstract:

Brain metastases are a common cause of death in stage IV metastatic melanoma. Dabrafenib is a BRAF inhibitor that has been developed to selectively target the valine 600 to glutamic acid substitution ($BRAF^{V600E}$) which is commonly found in metastatic melanoma. Clinical trials with dabrafenib are showing encouraging results, however the CNS distribution of dabrafenib remains unknown. Thus the objective of the current study was to evaluate the brain distribution of dabrafenib in mouse and to see whether active efflux by P-glycoprotein (P-gp) and Breast Cancer Resistance Protein (BCRP) restrict its delivery across blood-brain barrier (BBB). *In vitro* accumulation studies conducted in Madin-Darby canine kidney II (MDCKII) cells indicate that dabrafenib is an avid substrate for both P-gp and BCRP. Directional flux studies revealed greater transport in basolateral to apical direction with corrected efflux ratios of greater than 2 for both P-gp and Bcrp1 transfected cell lines. *In vivo,* the Kp (AUC_{brain} / AUC_{plasma}) of dabrafenib after an iv dose (2.5 mg/kg) was 0.023, which increased by 18-fold in Mdr1 *a/b*$^{-/-}$*Bcrp1*$^{-/-}$ mice to 0.42. Dabrafenib plasma exposure was ~2-fold greater in Mdr1 *a/b*$^{-/-}$*Bcrp1*$^{-/-}$ mice as compared to wild-type with an oral dose (25 mg/kg), however the brain distribution was increased by ~10-fold with a resulting Kp of 0.25. Further, compared to vemurafenib, another $BRAF^{V600E}$ inhibitor, dabrafenib has greater brain penetration with a similar dose. In conclusion, the dabrafenib brain distribution is limited in an intact BBB model and the data presented herein may have clinical implications in the prevention and treatment of melanoma brain metastases.

JPET Fast Forward. Published on December 17, 2012 as DOI: 10.1124/jpet.112.201475
This article has not been copyedited and formatted. The final version may differ from this version.

INTRODUCTION:

Melanoma is the most aggressive form of skin cancer as it accounts for more than 80% of deaths due to skin cancer. The incidence of melanoma has greatly increased over the past decade (Siegel et al., 2011). Extensive data in the literature point to the key role of mitogen-activated protein kinase (MAPK) pathway in melanoma pathogenesis. The MAPK pathway is involved in regulation of melanoma cell proliferation, growth, and survival. The downstream effectors of this signaling cascade include RAS-RAF-MEK-ERK (McCubrey et al., 2008). BRAF is a commonly mutated protein in melanoma, with ~80% carrying a V600E ($BRAF^{V600E}$) mutation (Davies et al., 2002). Thus, targeting this pathway represents an attractive therapeutic approach for melanoma.

Until recently, treatment options for melanoma were limited with no improvement in overall survival rates (Tsao et al., 2004; Garbe et al., 2011). However, in recent years there has been a tremendous improvement in the treatment of melanoma. Targeting $BRAF^{V600E}$ has proved to be a major advancement in the field of melanoma treatment (Flaherty et al., 2012; Sosman et al., 2012). For example, the recently US FDA approved drug, vemurafenib, a $BRAF^{V600E}$ inhibitor, showed remarkable efficacy against peripheral metastases (Chapman et al., 2011). However, brain metastases are prevalent in stage IV metastatic melanoma. This situation is alarming because ~50-75% of melanomas metastasize to the brain (Fife et al., 2004), and among those patients who have brain metastases, ~90% succumb to death (Skibber et al., 1996). The efficacy of vemurafenib in brain metastases of melanoma is under clinical investigation. Recent preclinical studies have indicated that vemurafenib distribution is restricted at blood-brain barrier (BBB) (Durmus et al., 2012; Mittapalli et al., 2012).

Dabrafenib (GSK2118436A, **Figure 1**) targets both $BRAF^{V600E}$ and $BRAF^{V600k}$. Dabrafenib showed very encouraging results in a phase 1 dose escalation study (Falchook et

al., 2012; Hauschild et al., 2012). The safety and clinical response of dabrafenib against peripheral metastases is comparable with that of vemurafenib, with an objective response of ~56% (Gibney and Sondak, 2012; Hauschild et al., 2012). Further, ~90% (9 out of 10 patients) of the patients with melanoma brain metastases had a reduction in tumor size (Falchook et al., 2012). However, important questions remain about the effective delivery to all sites of brain metastases, especially to the micro metastases which are situated beyond an intact blood-brain barrier (BBB). In a recent study, using preclinical model of brain metastases from breast cancer, it was shown that the blood-tumor barrier remains a significant impediment to chemotherapeutic drugs (Lockman et al., 2010). However, to date there are no data available in terms of drug delivery to brain metastases of melanoma. Further, it was shown that treatment of peripheral disease with targeted therapy increases the incidence of brain metastases (Rochet et al., 2012). A phase 2 clinical trial evaluating the efficacy of dabrafenib in brain metastases of melanoma is underway (Long et al., 2012) (clinicaltrials.gov identifier: NCT01266967). With this perspective, it is imperative to study the brain distribution of dabrafenib to provide a rationale to support clinical trials.

A critical challenge in treating brain metastases or in fact any neurological disorder is the delivery of drugs to the central nervous system. The BBB, an interface between blood and the brain, helps maintain homeostasis of the CNS and protects the brain from harmful toxins, metals and infectious agents (Deeken and Loscher, 2007). Together with capillary endothelial cells and tight junctions, it acts as a physical barrier (Hawkins and Davis, 2005). Further, with the expression of active efflux transporters such as P-glycoprotein (P-gp) and breast cancer resistance protein (BCRP), it acts a functional barrier (Schinkel and Jonker, 2003). Several anticancer agents have been shown to be substrates for both P-gp and BCRP and as such the brain distribution of these molecules is limited because of active efflux at the BBB (de Vries et al., 2007; Polli et al., 2009; Agarwal et al., 2010; Agarwal et al., 2011; Mittapalli et al., 2012).

JPET Fast Forward. Published on December 17, 2012 as DOI: 10.1124/jpet.112.201475
This article has not been copyedited and formatted. The final version may differ from this version.

In our previous study, we have shown that the brain distribution of vemurafenib is severely restricted at BBB due to active efflux by both P-gp and BCRP (Mittapalli et al., 2012). Given the highly encouraging clinical results with dabrafenib, the aim of the present study was to evaluate the brain distribution of dabrafenib in mouse, with the hope that these preclinical data would help in further improvement of a durable response in melanoma brain metastases patients. Using both *in vitro* transport studies and *in vivo* pharmacokinetic studies, we show that dabrafenib is a substrate for both P-gp and Bcrp and as such its brain distribution is limited in an intact BBB model. The data presented herein have clinical implications in the prevention or treatment of melanoma brain metastases because of concerns that sub-therapeutic concentrations in the brain or at sites of micro metastases with an intact BBB would result in limited anti-tumor activity.

MATERIALS AND METHODS:

Chemicals: Dabrafenib (GSK2118436A) was purchased from Chemieteck (Indianapolis, IN). [^{3}H]-vinblastine and [^{3}H]-mitoxantrone were purchased from Moravek Biochemicals (La Brea, CA). [^{3}H]-prazosin was purchased from PerkinElmer Life and Analytical Sciences (Waltham, MA). [^{14}C]-Inulin was purchased from American Radiolabeled Chemicals, Inc. (St. Louis, MO). Ko143 was purchased from Tocris Bioscience (MO, USA). Zosuquidar [LY335979, (*R*)-4-((1*aR*, 6*R*,10*bS*)-1,2-difluoro-1,1*a*,6,10*b*-tetrahydrodibenzo-(*a*,*e*) cyclopropa (*c*)cycloheptan-6-yl)-((5-quinoloyloxy) methyl)-1-piperazine ethanol, trihydrochloride] was kindly provided Eli Lilly and Co.(Indianapolis, IN). All other chemicals used were of high performance liquid chromatography or reagent grade and were obtained from Sigma-Aldrich (St. Louis, MO).

In vitro studies:

Polarized Madin-Darby canine kidney II (MDCKII) cells were used for all the *in vitro* studies. MDCKII-Wild-type (WT) and Bcrp1-transfected (MDCKII-Bcrp1) cells were a kind gift from Dr.

Alfred Schinkel (The Netherlands Cancer Institute). MDCKII-WT and MDR1-transfected (MDCKII-MDR1) cell lines were kindly provided by Dr. Piet Borst (The Netherlands Cancer Institute). Cells were cultured in Dulbecco's modified Eagle's medium supplemented with 10% (v/v) fetal bovine serum and antibiotics (penicillin, 100 U/mL; streptomycin, 100 µg/mL; and amphotericin B, 250 ng/mL). Cells were grown in 25 mL tissue culture treated flasks before seeding for the experiments and were maintained at 37º C in a humidified incubator with 5% CO_2. The growth media for MDCKII-MDR1 additionally contained 80 ng/ml of colchicine to maintain positive selection pressure of P-gp expression.

In vitro cellular accumulation: Cellular accumulation studies were performed in 12-well polystyrene plates with a seeding density of 2 x 10^5 cells per well, and media was changed every other day until confluent monolayers are formed. The cells were washed two times with warm cell assay buffer (122 mM NaCl, 25 mM $NaHCO_3$, 10 mM glucose, 10 mM HEPES, 3 mM KCl, 2.5 mM $MgSO_4$, 1.8 mM $CaCl_2$, and 0.4 mM K_2HPO_4) on the day of the experiment, and preincubated with cell assay buffer for 30 min. The cell assay buffer was aspirated after pre-incubation period, and the experiment was initiated by adding one ml of 2 µM of dabrafenib to each well and further incubated for 60 min in an orbital shaker (60 rpm) that was maintained at 37º C. At the end of 60 min accumulation, the experiment was ended by aspirating the dabrafenib solution followed by washing twice with ice-cold PBS. Cell lysis was accomplished by adding 0.5 milliliters of 1 % Triton-X. When the inhibitor was present it was included in both pre-incubation and accumulation steps. The concentration of dabrafenib in solubilized cell fractions was analyzed using liquid chromatography-tandem mass spectrometry (LC-MS/MS) as described below, and was normalized to the protein content.

Bcrp and P-gp inhibition studies: Inhibition studies were performed using prototypical probe substrates, [^{3}H]-prazosin or [^{3}H]-mitoxantrone for Bcrp and [^{3}H]-vinblastine for P-gp. The

intracellular accumulation of these probe substrates was evaluated in presence of varying concentrations of dabrafenib ranging from 0.1 to 50 µM. Briefly, the cells were pre-incubated with increasing concentrations of dabrafenib for 30 min. After pre-incubation the cells were incubated with radiolabelled probe substrate along with increasing concentrations of dabrafenib for 60 min. At the end of the incubation period, the radiolabelled probe substrate was aspirated; cell lysis was accomplished using 1% Triton-X. The radioactivity in solubilized cell fractions was determined by liquid scintillation counting (LS-6500; Beckman Coulter, Fullerton, CA). The radioactivity in cell fractions was normalized to protein concentrations in each well. The increase in cellular accumulation of probe substrate as compared to control (no treatment with dabrafenib) was measured and reported as a function of dabrafenib concentration.

Directional flux studies: The bidirectional transport assays were performed in 12-well Transwell® plates (polyester membrane, 0.4 µM pore size, 1.12 cm^2 growth surface area; Corning Inc., USA). The cells were seeded at a density of 2 $x10^5$ cells per well and the media was changed every other day until confluent monolayers were formed. The monolayer tightness was assessed by measurement of trans-epithelial electrical resistance (TEER). In parallel, the cell monolayer integrity was evaluated by analyzing the leakage of [^{14}C]-Inulin using the same passage cells seeded on the same day and at the same density.

On the day of the experiment, the cell monolayers were washed with pre-warmed cell assay buffer and preincubated for 30 minutes after which the experiment was initiated by adding 5 µM of dabrafenib solution in cell assay buffer to the donor compartment. Samples (100 µL) were collected from receiver compartment at 60, 120, and 180 min and replaced immediately with drug-free cell assay buffer. In addition, at the beginning of the experiment, 100 µL of sample was collected from donor compartment and replaced with 100 µL drug solution. The Transwell® assay plates were incubated in an orbital shaker (60 rpm) maintained at 37 °C for the duration of experiment except for the brief sampling times. In the inhibition experiments,

JPET Fast Forward. Published on December 17, 2012 as DOI: 10.1124/jpet.112.201475
This article has not been copyedited and formatted. The final version may differ from this version.

either 0.2 µM Ko143 (selective Bcrp inhibitor) or 1 µM of zosuquidar (selective P-gp inhibitor) was added to both apical (A) and basolateral (B) compartments. Dabrafenib concentration was measured by LC-MS/MS. The apparent permeability (P_{app}), in A-to-B and B-to-A directions, was calculated as follows: P_{app} = (dQ/dt) (1/A x C_0), where dQ/dt is the slope obtained from the initial linear range from the amount transported versus time graph, A is the area of the Transwell® membrane, and C_0 is the initial donor concentration. The efflux ratio (ER) and the corrected efflux ratio (CFR) were calculated as follows: Efflux ratio = [P_{app} (B → A) / P_{app} (A → B)]; Corrected efflux ratio = (Efflux ratio in transfected cells) / (Efflux ratio in wild-type cells); where, A→B represents permeability in apical to basolateral and B→A represents permeability in basolateral to apical direction.

Equilibrium dialysis experiments: Unbound fractions in mouse plasma and brain homogenates were determined using equilibrium dialysis cassettes (Fisher Scientifc, Acrylic, 1mL) as described by Kalvass et.al. (Kalvass et al., 2007). For initial pilot studies commercial mouse plasma (Valley Biomedical, Winchester, VA) and pooled brain homogenates from wild-type and knockout mice were used to determine the time to reach the equilibrium (**Supplemental Fig. 3**). Once the time to reach equilibrium was determined, the free fraction experiments were performed in plasma and brains isolated freshly from either wild-type or *Mdr1a/b*$^{-/-}$*Bcrp1*$^{-/-}$ mice. Spectra/por® dialysis membranes (MWCO: 12-14000 Da; Spectrum Laboratories, Inc. CA) were equilibrated in HPLC-water for 30 min followed by 30 min in ECF buffer (pH 7.4). Three volumes of ECF buffer was added to the brain tissue and homogenized to get a uniform homegenate. Dabrafenib was added to plasma and brain homogenate to achieve a final concentration of 2 µM; 1 ml was (n =3) loaded into the equilibrium dialysis cassette and dialyzed against an equal volume of ECF buffer (pH 7.4) in an orbital shaker (200 rpm) maintained at 37 °C. Equilibrium was achieved in ~ 6 hrs in both plasma and brain homogenates (**Supplemental Fig. 3**). At the end of the experiment, matrix (plasma or brain

homogenate) and buffer samples were removed from dialysis cassette and the concentrations of dabrafenib were measured using LC-MS/MS.

In vivo studies:

All of the *in vivo* studies were performed in FVB (wild-type) and *Mdr1a/b*$^{-/-}$*Bcrp1*$^{-/-}$ (triple knockout) mice of either sex of a FVB genetic background (Taconic Farms, Germantown, NY). All animals were 8 to 10 weeks old at the time of experiment. Animals were maintained in a 12 hr light/dark cycle with an unlimited access to food and water. All studies were carried out in accordance with the guidelines set by the *Principles of Laboratory Animal Care* (National Institutes of Health, Bethesda, MD) and approved by the Institutional Animal Care and Use Committee of the University of Minnesota.

Plasma and brain pharmacokinetics of dabrafenib after intravenous and oral administration: All dosing formulations of dabrafenib were prepared on the day of the experiment. Dabrafenib dosing formulations were prepared either as a solution in a vehicle containing DMSO, propylene glycol, and water (40:40:20; for i.v. dosing studies) or as a stable suspension in 1% carboxy methyl cellulose (for oral dosing studies).

In the first study, FVB wild-type and *Mdr1a/b*$^{-/-}$*Bcrp1*$^{-/-}$ mice were administered an i.v. dose of 2.5 mg/kg via the tail vein. Blood and brain samples were collected 5, 15, 30, 60, and 120 min post dose (n =4 at each time point). Animals were euthanized using a CO_2 chamber at the desired time point. Blood was collected by cardiac puncture and plasma was harvested. Whole brain was removed from the skull and washed with ice-cold PBS; superficial meninges were removed by blotting with tissue paper. Plasma and brain specimens were stored at -80° C until further analysis.

In another study, FVB wild-type and *Mdr1a/b*$^{-/-}$*Bcrp1*$^{-/-}$ mice were administered 25 mg/kg dabrafenib via oral gavage. Blood and brain samples were harvested at 15, 30, 60, 120, and

240 min post dose (n =4 at each time point) as described above. Brain concentrations were corrected for residual drug in brain vasculature assuming a vascular volume of 1.4% in mouse brain (Dai et al., 2003).

LC-MS/MS Analysis: The concentrations of dabrafenib from all *in vitro* and *in vivo* studies were determined using a specific and sensitive LC-MS/MS assay. Brain samples were thawed to room temperature and homogenized with three volumes of 5% bovine serum albumin in PBS. An aliquot of sample (cell lysate, cell assay buffer, plasma, or brain homogenate) was spiked with 10 ng of internal standard [AG1478; (4-(3-chloroanilino)-6,7-dimethoxyquinazoline)] and liquid-liquid extraction was performed by addition of 10 volumes of ethyl acetate. After extraction, the supernatant organic layer was transferred to a micro-centrifuge tube and dried under gentle stream of nitrogen. The dried sample was reconstituted in 100 µL of mobile phase, vortex-mixed, centrifuged, transferred to auto sampler vials, and a 5 µL sample was injected onto the column, a Zorbax Eclipse XDB-C18 column (4.6 x 50 mm, 1.8 µm particle size; Agilent Technologies, Santa Clara, CA). The aqueous mobile phase (A) was 20 mM ammonium formate with 0.1% formic acid and the organic mobile phase (B) was acetonitrile. The gradient was as follows: 50% B for the first 3 min, and increased to 90% B from 3 to 3.5 min and maintained at 90% B for 3 min, and decreased to 50% B within 0.5 min. The total run time was 11 min with a flow rate of 0.35 mL/min. The ionization was conducted in positive mode and the m/z transitions were 520.122 → 307.007, and 316.068 → 299.993 for dabrafenib and AG1478, respectively. The retention time of dabrafenib was 6.8 min and that of AG1478 was 2.8 min. The assay was sensitive and linear over a range of 2 ng/mL to 2 µg/mL, with the coefficient of variation being less than 20% over the entire range.

Pharmacokinetic calculations: Pharmacokinetic parameters and metrics from the concentration-time data in plasma and brain were obtained by non-compartmental analysis

(NCA) performed using Phoenix WinNonlin 6.2 (Mountain View, CA). The area under the concentration-time profiles for plasma (AUC_{plasma}) and brain (AUC_{brain}) were calculated using the linear trapezoidal method. The sparse sampling module in WinNonlin 6.2 (Pharsight, Mountain View, CA) was used to estimate the standard error around the mean of the AUCs (Bailer, 1988; Nedelman et al., 1995).

Statistical Analysis: Data in all experiments represent mean ± SD unless otherwise indicated. One way ANOVA, followed by Bonferonni's multiple comparisons test, was utilized to compare multiple groups. Comparisons between two groups were made using an unpaired t-test. A significance level of $p < 0.05$ was used for all experiments. (Graph Pad Prism 5.01 software, San Diego, CA, USA).

RESULTS:

In vitro accumulation of dabrafenib in MDCKII-Bcrp1 and MDCKII-MDR1 cells: The cellular accumulation of dabrafenib in MDCKII- wild-type, Bcrp1, and MDR1 transfected cell lines is summarized in **Fig. 2**. [^{3}H]-prazosin and [^{3}H]-vinblastine were used as positive controls for Bcrp and MDR1, respectively, and as expected, the cellular accumulation of these probe substrates were significantly lower as compared to wild-type controls [WT: (100 ± 8); Bcrp1: (16.7 ± 1.4); MDR1: (11.6 ± 3.1);] confirming significant transporter activity in these transfected cell lines. We choose a concentration of 2 µM for dabrafenib accumulation studies as the pilot studies revealed that no saturation of transporters occur up to 75 µM of dabrafenib (**Supplemental Fig. 1**). Dabrafenib accumulation was significantly lower in Bcrp1 cells [**Fig. 2A,** Bcrp: (11.3 ± 1.4); WT: (100 ± 10); $p < 0.001$] when compared to corresponding wild-type controls. The addition of 0.2 µM of Ko143, a specific Bcrp1 inhibitor, increased dabrafenib accumulation, such that it was not significantly different than wild-type control. Likewise, dabrafenib accumulation in MDR1

JPET Fast Forward. Published on December 17, 2012 as DOI: 10.1124/jpet.112.201475
This article has not been copyedited and formatted. The final version may differ from this version.

transfected cell lines (**Fig. 2B**) was ~ 65% lower when compared wild-type control and the difference was abolished when 1 μM of LY335979 was used. These data indicate that dabrafenib is a substrate for both P-gp and Bcrp1 and inhibition of these efflux transporters enhance the cellular delivery of dabrafenib.

Competition assays using prototypical probe substrates: The effect of increasing concentrations of dabrafenib on the cellular accumulation of prototypical probe substrates (prazosin or mitoxantrone for Bcrp, vinblastine for P-gp) was assessed in MDCKII-wild-type, Bcrp1 and MDR1 transfected cell lines. Increasing concentrations of dabrafenib did not increase the accumulation of [^{3}H]-prazosin in both Bcrp cells as well as the respective wild-type control cells (**Fig. 3A**). Similarly, increasing dabrafenib concentrations did not increase the accumulation of [^{3}H]-vinblastine until 25 μM was reached, however at 50 μM of dabrafenib, there was ~1.5 and 2.5 fold increase in vinblastine accumulation in wild-type and MDR1 cells, respectively (**Fig. 3B**). Furthermore, dabrafenib did not change the cellular accumulation of mitoxantrone in Bcrp1 cells (**Supplemental Fig. 2**).

Directional transport studies: The directional transport of dabrafenib was assessed using monolayers of MDCKII-wild-type, Bcrp1, and MDR1 transfected lines grown on Transwell® permeable membranes. Confluent monolayers were formed in 3 to 4 days with intact tight junctions. Paracellular leakage was assessed by measuring the transport of [^{14}C]-Inulin across the cell monolayers and the inulin transported in 60 min was found to be less than 1%. The directional permeability of dabrafenib was very similar between A-to-B and B-to-A directions in the wild-type cells (11.5 ± 1.4 vs 14.1 ± 1.4 x 10^{-6} cm/s for A-to-B and B-to-A, respectively; **Table 1**). However in the Bcrp1 transfected cell line, the apparent permeability of dabrafenib in B-to-A direction was significantly higher than the permeability in A-to-B direction [A-to-B: (1.3 ± 0.3); B-to-A: 27.3 ± 4.1), $p < 0.05$; **Table 1**) with and efflux ratio of 21. Treatment with Ko143 significantly ($p < 0.05$) reduced the Bcrp1-mediated efflux of dabrafenib in B-to-A direction and

JPET Fast Forward. Published on December 17, 2012 as DOI: 10.1124/jpet.112.201475
This article has not been copyedited and formatted. The final version may differ from this version.

increased the A-to-B permeability with a resulting efflux ratio of 0.7. The corrected efflux ratio was found to be ~18 for Bcrp1 mediated transport. Similarly, in MDR1 cells the B-to-A permeability was significantly higher compared to A-to-B permeability with an efflux ratio of 11. Addition of LY335979, a specific P-gp inhibitor, abolished the difference in directional permeabilities with a resulting efflux ratio of 1 (**Table 2**). The corrected efflux ratio was ~4. These results conclusively indicate that dabrafenib is an avid substrate for both Bcrp1 and P-gp.

Plasma protein and brain tissue binding: Since it is the unbound drug concentration that results in pharmacological action, we determined the free fraction (f_u) in plasma and brain tissue homogenates. Dabrafenib is highly bound to plasma proteins as well as brain tissue. No significant difference was observed in free fraction in plasma and brain tissue homogenate when compared between wild-type and *Mdr1a/b*$^{-/-}$*Bcrp1*$^{-/-}$ mice genotypes [Wild-type: ($f_{u,\ plasma}$ = 0.004 ± 0.001), ($f_{u,brain\ homogenate}$ = 0.02 ± 0.003); *Mdr1a/b*$^{-/-}$*Bcrp1*$^{-/-}$: ($f_{u,\ plasma}$ = 0.006 ± 0.004), ($f_{u,brain\ homogenate}$ = 0.02 ± 0.005)].

Brain distribution of dabrafenib in FVB wild-type and Mdr1a/b*$^{-/-}$*Bcrp1*$^{-/-}$ *mice: The brain and plasma dabrafenib concentration time profiles after an i.v. dose of 2.5 mg/kg in FVB wild-type mice are summarized in **Fig. 4**. The brain concentrations of dabrafenib were significantly lower than the corresponding plasma concentrations at all measured time points. The pharmacokinetic parameters were summarized in **Table 3**. The brain-to-plasma partitioning (K_p, AUC_{brain} / AUC_{plasma}) was found to be 0.023, indicating the limited distribution of dabrafenib to the brain. We also investigated the brain distribution of dabrafenib in *Mdr1a/b*$^{-/-}$*Bcrp1*$^{-/-}$ mice after a 2.5 mg/kg i.v. dose of dabrafenib. The plasma concentrations were no different between wild-type and *Mdr1a/b*$^{-/-}$*Bcrp1*$^{-/-}$ mice (**Fig. 5A**), however the brain concentrations of dabrafenib in *Mdr1a/b*$^{-/-}$*Bcrp1*$^{-/-}$ mice (**Fig. 5B**) were significantly higher than the corresponding brain concentrations observed in wild-type mice. The K_p in *Mdr1a/b*$^{-/-}$*Bcrp1*$^{-/-}$ mice increased to ~0.4

JPET Fast Forward. Published on December 17, 2012 as DOI: 10.1124/jpet.112.201475
This article has not been copyedited and formatted. The final version may differ from this version.

which was 18-fold greater than what was observed in wild-type mice indicating the influence of P-gp, Bcrp or both on the brain distribution of dabrafenib.

Dabrafenib is administered to patients orally (Falchook et al., 2012) and we sought to determine the brain and plasma pharmacokinetics after an oral dose. Hence, in a separate study, we investigated the brain distribution of dabrafenib after an oral dose of 25 mg/kg in wild-type and *Mdr1a/b*$^{-/-}$*Bcrp1*$^{-/-}$ mice, and the results are summarized in **Fig. 6** and **Table 4**. The AUC_{plasma} in *Mdr1a/b*$^{-/-}$*Bcrp1*$^{-/-}$ mice (31 ± 5 µg x min/mL) was ~2-fold higher as compared to the wild-type mice (16 ± 3 µg x min/mL). This indicates that P-gp and Bcrp may have some influence on the oral absorption or systemic clearance of dabrafenib at 25 mg/kg dose. Dabrafenib brain concentrations were significantly enhanced in *Mdr1a/b*$^{-/-}$*Bcrp1*$^{-/-}$ mice compared with those in wild-type. The AUC_{brain} in wild-type mice was 0.69 µg x min/mL which increased approximately 10-fold in *Mdr1a/b*$^{-/-}$*Bcrp1*$^{-/-}$ to 7.6 µg x min/mL. The K_p in wild-type mice was 0.044, which increased by 6 fold in *Mdr1a/b*$^{-/-}$*Bcrp1*$^{-/-}$ mice to 0.25. The aggregate of these data suggests that the brain distribution of dabrafenib is significantly limited at BBB due to active efflux by both P-gp and BCRP after either intravenous or oral administration.

Comparison of brain distribution of dabrafenib with vemurafenib: We compared the brain distribution of dabrafenib after single oral dose with our previously published results for vemurafenib (Mittapalli et al., 2012) and the data were shown in **Fig. 7**. The plasma concentrations, for both dabrafenib and vemurafenib, were higher in the *Mdr1a/b*$^{-/-}$*Bcrp1*$^{-/-}$ mice as compared to wild-type mice (**Fig. 7A**). It should be noted that the plasma concentrations of dabrafenib were not significantly different as compared to vemurafenib in either type of the mice. Since the total brain distribution of vemurafenib was approximately equal to the brain vascular volume, for comparison purposes, the data shown in this particular case was not corrected for vascular content for both dabrafenib and vemurafenib. The brain concentrations of dabrafenib were significantly higher as compared to vemurafenib brain concentrations in both

JPET Fast Forward. Published on December 17, 2012 as DOI: 10.1124/jpet.112.201475
This article has not been copyedited and formatted. The final version may differ from this version.

wild-type and *Mdr1a/b*$^{-/-}$*Bcrp1*$^{-/-}$ mice (**Fig. 7B**). The brain-to-plasma concentration ratio for dabrafenib is ~10, ~4 fold greater compared to vemurafenib brain to plasma ratio in wild-type and *Mdr1a/b*$^{-/-}$*Bcrp1*$^{-/-}$ mice, respectively [Wild-type: dabrafenib: (0.1 ± 0.03); vemurafenib: (0.008 ± 0.001); *Mdr1a/b*$^{-/-}$*Bcrp1*$^{-/-}$: dabrafenib: (0.3 ± 0.04); vemurafenib: (0.07 ± 0.02);]. The aggregate of these data indicate that dabrafenib has greater brain penetration than vemurafenib.

DISCUSSION:

Brain metastases are a common cause of death from stage IV metastatic melanoma (Skibber et al., 1996; Davies et al., 2011). Until 2011, the only FDA approved therapies for metastatic melanoma were dacarbazine and interleukin-2, which showed response rates of only 10-20% (Comis, 1976; Atkins et al., 1999; Garbe et al., 2011). However, therapies for metastatic melanoma have been changed dramatically with the development of highly selective inhibitors of BRAF^{V600E}, the most commonly found mutation in melanoma patients. The first of these selective BRAF^{V600E} inhibitors, vemurafenib was approved by US FDA in 2011, and showed remarkable efficacy in clinical trials (Chapman et al., 2011). A second BRAF^{V600E} inhibitor, dabrafenib, showed similar results when compared to vemurafenib, with fewer adverse effects in clinical trials (Falchook et al., 2012; Hauschild et al., 2012). Further, dabrafenib showed remarkable efficacy in reducing the tumor size in brain of patients with brain metastases (Falchook et al., 2012). However, a durable response depends on effective delivery of therapies to all the sites of metastases in brain, especially to the micrometastases (less than 1 mm in diameter) that have an intact BBB (Gibney and Sondak, 2012) with functional efflux transporters. Furthermore, in a recent study, Rochet and colleagues reported that treatment of melanoma patients with vemurafenib resulted in development of metastatic disease in the brain (Rochet et al., 2012). From these data, it appears that the brain remains at least in part a

pharmacological sanctuary site due to the continued presence of an intact BBB where some metastatic sites reside. The efficacy of dabrafenib in brain metastases of melanoma is under investigation in a phase 2 clinical trial. With this perspective, it is critical to determine the mechanisms that limit the brain distribution of dabrafenib. In the current study, using both *in vitro* and *in vivo* models, we demonstrate that dabrafenib is a dual substrate for BCRP and P-gp and its brain distribution is limited due to active efflux at the BBB. Furthermore, our data indicate that dabrafenib has greater brain distribution when compared to vemurafenib and as such dabrafenib might have some advantages for treating patients with melanoma brain metastases. To the best of our knowledge, this is the first report to show the brain distribution of dabrafenib and its interactions with Bcrp and P-gp.

The experiments performed in transfected MDCKII cells that overexpress either murine Bcrp or human P-gp revealed that dabrafenib is a dual substrate for both Bcrp and P-gp (**Fig. 2, Tables 1** and **2**). Interestingly, inhibition studies conducted using prototypical probe substrates (prazosin and mitoxantrone for Bcrp, and vinblastine for P-gp) showed no increase in probe substrate accumulation with increasing concentrations of dabrafenib up to a concentration of 50 and 25 μM in Bcrp1 and MDR1 cells, respectively. In both wild-type and MDR1 cells, using vinblastine as a probe substrate, dabrafenib showed significant increase in accumulation at 50 μM. However, it should be noted that this concentration is not pharmacologically relevant, as the clinically observed concentrations of dabrafenib (given 150 mg/kg twice daily) are ~ 2 μM (Falchook et al., 2012).

It should be noted that specific Bcrp (Ko143) and P-gp (LY335979) inhibitors were able to increase cellular accumulation of dabrafenib (**Fig. 2**), as well as the probe substrates (**Fig. 3**), in both Bcrp1 and MDR1 cells, respectively, indicating that Ko143 and LY335979 bind to multiple binding sites on the transporter proteins. The fact that dabrafenib is a substrate for both Bcrp and P-gp, but does not inhibit these transporter proteins for some prototypical probe substrates, may indicate that dabrafenib is binding to a different site on the transporter protein

JPET Fast Forward. Published on December 17, 2012 as DOI: 10.1124/jpet.112.201475
This article has not been copyedited and formatted. The final version may differ from this version.

as compared to the probe substrates tested. It is noteworthy to recognize how screening assays using specific binding site probe substrates can be misleading. In our previous studies, we have shown that differences exist in the inhibition of BCRP depending on both the inhibitor used and the substrate under evaluation (Giri et al., 2009).

With this knowledge from *in vitro* data, we next investigated the *in vivo* brain distribution of dabrafenib in mouse. After an i.v. dose, the brain concentrations of dabrafenib in FVB wild-type mice were significantly lower than the corresponding plasma concentrations (**Fig. 4**), with a K_p of 0.023. However, the brain distribution of dabrafenib was significantly improved when the same dose was administered in *Mdr1a/b*$^{-/-}$*Bcrp1*$^{-/-}$ mice, with a resulting K_p of 0.42 (**Table 3**). It is worth noting that the unbound brain-to-plasma partition ratio (K_p,uu) in wild-type and *Mdr1a/b*$^{-/-}$ *Bcrp1*$^{-/-}$ mice were ~0.1 and ~1.7, respectively. These data indicate that dabrafenib brain distribution is limited in an intact BBB model through the action of efflux transporter mediated clearance.

Since the clinical use of dabrafenib utilizes chronic oral dosing, we next determined the brain distribution of dabrafenib after oral administration. The AUC_{plasma} in *Mdr1a/b*$^{-/-}$*Bcrp1*$^{-/-}$ mice is ~2-fold higher (**Fig. 6A; Table 4**) as compared to wild-type mice after oral administration. As the systemic clearance is no different between the genotypes after an i.v. dose (see **Fig.5; Table 3**), the observed higher plasma exposure in Mdr1a/b-/-Bcrp1-/- mice after oral dose indicate that BCRP and P-gp may have some influence on oral absorption of dabrafenib at 25 mg/kg dose. This phenomenon was observed with other drugs that are dual substrates of BCRP and P-gp, such as dasatinib (Lagas et al., 2009) and vemurafenib (Durmus et al., 2012). However the brain concentrations are ~12-fold higher in *Mdr1a/b*$^{-/-}$*Bcrp1*$^{-/-}$ mice resulting in a ~6-fold increase in B/P ratio as compared to wild-type mice. Taken together, all these data indicate that dabrafenib brain distribution is limited in an intact BBB model. In this regard, use of pharmacological inhibitors such as elacridar, a dual P-gp and Bcrp inhibitor, may have significant value in improving the CNS distribution of dabrafenib.

JPET Fast Forward. Published on December 17, 2012 as DOI: 10.1124/jpet.112.201475
This article has not been copyedited and formatted. The final version may differ from this version.

Since both dabrafenib and vemurafenib are showing remarkable results in clinical trials, it is appropriate to compare these two molecules in terms of their brain distribution. In our previous study, we have shown that both BCRP and P-gp have a significant impact on the brain distribution of vemurafenib (Mittapalli et al., 2012), which was further supported by a recently published report by another group (Durmus et al., 2012). Compared to vemurafenib (Mittapalli et al., 2012) the B/P ratio of dabrafenib is significantly higher in both wild-type and *Mdr1a/b*$^{-/-}$*Bcrp1*$^{-/-}$ mice (**Fig. 7**). While the B/P ratio in this case was measured only at one time point, we also observed a greater AUC_{brain} to AUC_{plasma} of dabrafenib in wild-type mice after a similar i.v. dose as compared vemurafenib (**Table 5**). Given the *in vitro* potency of dabrafenib, which is at least 40 times higher than vemurafenib against $BRAF^{V600E}$ [vemurafenib IC_{50}: 31 nM (Bollag et al., 2010); dabrafenib IC_{50}: 0.8 nM (Laquerre et al., 2009)], and greater brain penetration than vemurafenib, dabrafenib might be beneficial in treating melanoma brain metastases, however this prediction warrants further preclinical and clinical investigation.

Currently, the duration of response with single agent therapy has been limited because the development of resistance is inevitable, as reported in case of vemurafenib (Johannessen et al., 2010; Nazarian et al., 2010; Villanueva et al., 2010). Further, studies have shown that mutations in upstream signaling proteins such as RAS or compensatory signaling from other growth factor receptors such as PI3K/mTOR drive the reactivation of the MAPK signaling pathway and build up the resistance to BRAF therapy (Flaherty et al., 2012). Thus, understanding the key molecular aberrations associated with resistance will be crucial in designing the rational combinations using two or more drugs to simultaneously block multiple pathways, such as the clinical trial evaluating the combination of dabrafenib with the MEK inhibitor trametinib (NCT01072175). Also, the evaluation of combinations of immune therapies such as ipilimumab (Margolin et al., 2012) and rational choices of molecularly-targeted agents would be valuable in overcoming the low response rates of immune therapy and short durations of response associated with targeted therapies.

The development of $BRAF^{V600E}$ inhibitors has been a major breakthrough for the treatment of melanoma patients. However, challenges still remain in delivering these targeted therapies to melanoma micro metastases in brain that could be growing behind an intact BBB. Given the success rate so far with both dabrafenib and vemurafenib, it will be essential to determine the both the resistance mechanisms and CNS delivery issues that need to be addressed to achieve a durable response. Multiple drugs / cocktails need to be evaluated for rational combinations (e.g., a BRAF inhibitor and/or MEK inhibitor and/or PI3K/mTOR inhibitor) to decrease resistance in peripheral or systemic disease. At the same time, there is also a critical need to examine the CNS delivery of combinations to see if one agent influences the brain delivery of another, or one or more drug(s) in the combination does not reach the brain, leading to heightened resistance. The successful and durable treatment of melanoma requires that the brain does not become a pharmacological sanctuary site for melanoma metastases.

Acknowledgments:

The authors thank Jim Fisher, Clinical Pharmacology Analytical Services Laboratory, University of Minnesota, for help and support in the development of the dabrafenib LC-MS/MS assay.

Authorship Contributions

Participated in research design: Mittapalli, Vaidhyanathan, Dudek, and Elmquist

Conducted experiments: Mittapalli, Vaidhyanathan

Performed data analysis: Mittapalli, Elmquist

Wrote or contributed to writing of the manuscript: Mittapalli, Dudek, and Elmquist

References:

Agarwal S, Sane R, Gallardo JL, Ohlfest JR and Elmquist WF (2010) Distribution of gefitinib to the brain is limited by P-glycoprotein (ABCB1) and breast cancer resistance protein (ABCG2)-mediated active efflux. *J Pharmacol Exp Ther* **334**:147-155.

Agarwal S, Sane R, Ohlfest JR and Elmquist WF (2011) The role of the breast cancer resistance protein (ABCG2) in the distribution of sorafenib to the brain. *J Pharmacol Exp Ther* **336**:223-233.

Atkins MB, Lotze MT, Dutcher JP, Fisher RI, Weiss G, Margolin K, Abrams J, Sznol M, Parkinson D, Hawkins M, Paradise C, Kunkel L and Rosenberg SA (1999) High-dose recombinant interleukin 2 therapy for patients with metastatic melanoma: analysis of 270 patients treated between 1985 and 1993. *J Clin Oncol* **17**:2105-2116.

Bailer AJ (1988) Testing for the equality of area under the curves when using destructive measurement techniques. *J Pharmacokinet Biopharm* **16**:303-309.

Bollag G, Hirth P, Tsai J, Zhang J, Ibrahim PN, Cho H, Spevak W, Zhang C, Zhang Y, Habets G, Burton EA, Wong B, Tsang G, West BL, Powell B, Shellooe R, Marimuthu A, Nguyen H, Zhang KY, Artis DR, Schlessinger J, Su F, Higgins B, Iyer R, D'Andrea K, Koehler A, Stumm M, Lin PS, Lee RJ, Grippo J, Puzanov I, Kim KB, Ribas A, McArthur GA, Sosman JA, Chapman PB, Flaherty KT, Xu X, Nathanson KL and Nolop K (2010) Clinical efficacy of a RAF inhibitor needs broad target blockade in BRAF-mutant melanoma. *Nature* **467**:596-599.

Chapman PB, Hauschild A, Robert C, Haanen JB, Ascierto P, Larkin J, Dummer R, Garbe C, Testori A, Maio M, Hogg D, Lorigan P, Lebbe C, Jouary T, Schadendorf D, Ribas A, O'Day SJ, Sosman JA, Kirkwood JM, Eggermont AM, Dreno B, Nolop K, Li J, Nelson B, Hou J, Lee RJ, Flaherty KT and McArthur GA (2011) Improved survival with vemurafenib in melanoma with BRAF V600E mutation. *N Engl J Med* **364**:2507-2516.

Comis RL (1976) DTIC (NSC-45388) in malignant melanoma: a perspective. *Cancer Treat Rep* **60**:165-176.

Dai H, Marbach P, Lemaire M, Hayes M and Elmquist WF (2003) Distribution of STI-571 to the brain is limited by P-glycoprotein-mediated efflux. *J Pharmacol Exp Ther* **304**:1085-1092.

Davies H, Bignell GR, Cox C, Stephens P, Edkins S, Clegg S, Teague J, Woffendin H, Garnett MJ, Bottomley W, Davis N, Dicks E, Ewing R, Floyd Y, Gray K, Hall S, Hawes R, Hughes J, Kosmidou V, Menzies A, Mould C, Parker A, Stevens C, Watt S, Hooper S, Wilson R, Jayatilake H, Gusterson BA, Cooper C, Shipley J, Hargrave D, Pritchard-Jones K, Maitland N, Chenevix-Trench G, Riggins GJ, Bigner DD, Palmieri G, Cossu A,

Flanagan A, Nicholson A, Ho JW, Leung SY, Yuen ST, Weber BL, Seigler HF, Darrow TL, Paterson H, Marais R, Marshall CJ, Wooster R, Stratton MR and Futreal PA (2002) Mutations of the BRAF gene in human cancer. *Nature* **417**:949-954.

Davies MA, Liu P, McIntyre S, Kim KB, Papadopoulos N, Hwu WJ, Hwu P and Bedikian A (2011) Prognostic factors for survival in melanoma patients with brain metastases. *Cancer* **117**:1687-1696.

de Vries NA, Zhao J, Kroon E, Buckle T, Beijnen JH and van Tellingen O (2007) P-glycoprotein and breast cancer resistance protein: two dominant transporters working together in limiting the brain penetration of topotecan. *Clin Cancer Res* **13**:6440-6449.

Deeken JF and Loscher W (2007) The blood-brain barrier and cancer: transporters, treatment, and Trojan horses. *Clin Cancer Res* **13**:1663-1674.

Durmus S, Sparidans RW, Wagenaar E, Beijnen JH and Schinkel AH (2012) Oral Availability and Brain Penetration of the B-RAF(V600E) Inhibitor Vemurafenib Can Be Enhanced by the P-Glycoprotein (ABCB1) and Breast Cancer Resistance Protein (ABCG2) Inhibitor Elacridar. *Mol Pharm*.

Falchook GS, Long GV, Kurzrock R, Kim KB, Arkenau TH, Brown MP, Hamid O, Infante JR, Millward M, Pavlick AC, O'Day SJ, Blackman SC, Curtis CM, Lebowitz P, Ma B, Ouellet D and Kefford RF (2012) Dabrafenib in patients with melanoma, untreated brain metastases, and other solid tumours: a phase 1 dose-escalation trial. *Lancet* **379**:1893-1901.

Fife KM, Colman MH, Stevens GN, Firth IC, Moon D, Shannon KF, Harman R, Petersen-Schaefer K, Zacest AC, Besser M, Milton GW, McCarthy WH and Thompson JF (2004) Determinants of outcome in melanoma patients with cerebral metastases. *J Clin Oncol* **22**:1293-1300.

Flaherty KT, Infante JR, Daud A, Gonzalez R, Kefford RF, Sosman J, Hamid O, Schuchter L, Cebon J, Ibrahim N, Kudchadkar R, Burris HA, 3rd, Falchook G, Algazi A, Lewis K, Long GV, Puzanov I, Lebowitz P, Singh A, Little S, Sun P, Allred A, Ouellet D, Kim KB, Patel K and Weber J (2012) Combined BRAF and MEK Inhibition in Melanoma with BRAF V600 Mutations. *N Engl J Med*.

Garbe C, Eigentler TK, Keilholz U, Hauschild A and Kirkwood JM (2011) Systematic review of medical treatment in melanoma: current status and future prospects. *Oncologist* **16**:5-24.

Gibney GT and Sondak VK (2012) Extending the reach of BRAF-targeted cancer therapy. *Lancet* **379**:1858-1859.

Giri N, Agarwal S, Shaik N, Pan G, Chen Y and Elmquist WF (2009) Substrate-dependent breast cancer resistance protein (Bcrp1/Abcg2)-mediated interactions: consideration of multiple binding sites in in vitro assay design. *Drug Metab Dispos* **37**:560-570.

Hauschild A, Grob JJ, Demidov LV, Jouary T, Gutzmer R, Millward M, Rutkowski P, Blank CU, Miller WH, Jr., Kaempgen E, Martin-Algarra S, Karaszewska B, Mauch C, Chiarion-Sileni V, Martin AM, Swann S, Haney P, Mirakhur B, Guckert ME, Goodman V and Chapman PB (2012) Dabrafenib in BRAF-mutated metastatic melanoma: a multicentre, open-label, phase 3 randomised controlled trial. *Lancet* **380**:358-365.

Hawkins BT and Davis TP (2005) The blood-brain barrier/neurovascular unit in health and disease. *Pharmacol Rev* **57**:173-185.

Johannessen CM, Boehm JS, Kim SY, Thomas SR, Wardwell L, Johnson LA, Emery CM, Stransky N, Cogdill AP, Barretina J, Caponigro G, Hieronymus H, Murray RR, Salehi-Ashtiani K, Hill DE, Vidal M, Zhao JJ, Yang X, Alkan O, Kim S, Harris JL, Wilson CJ, Myer VE, Finan PM, Root DE, Roberts TM, Golub T, Flaherty KT, Dummer R, Weber BL, Sellers WR, Schlegel R, Wargo JA, Hahn WC and Garraway LA (2010) COT drives resistance to RAF inhibition through MAP kinase pathway reactivation. *Nature* **468**:968-972.

Kalvass JC, Maurer TS and Pollack GM (2007) Use of plasma and brain unbound fractions to assess the extent of brain distribution of 34 drugs: comparison of unbound concentration ratios to in vivo p-glycoprotein efflux ratios. *Drug Metab Dispos* **35**:660-666.

Lagas JS, van Waterschoot RA, van Tilburg VA, Hillebrand MJ, Lankheet N, Rosing H, Beijnen JH and Schinkel AH (2009) Brain accumulation of dasatinib is restricted by P-glycoprotein (ABCB1) and breast cancer resistance protein (ABCG2) and can be enhanced by elacridar treatment. *Clin Cancer Res* **15**:2344-2351.

Lockman PR, Mittapalli RK, Taskar KS, Rudraraju V, Gril B, Bohn KA, Adkins CE, Roberts A, Thorsheim HR, Gaasch JA, Huang S, Palmieri D, Steeg PS and Smith QR (2010) Heterogeneous blood-tumor barrier permeability determines drug efficacy in experimental brain metastases of breast cancer. *Clin Cancer Res* **16**:5664-5678.

Long GV, Trefzer U, Davies MA, Kefford RF, Ascierto PA, Chapman PB, Puzanov I, Hauschild A, Robert C, Algazi A, Mortier L, Tawbi H, Wilhelm T, Zimmer L, Switzky J, Swann S, Martin AM, Guckert M, Goodman V, Streit M, Kirkwood JM and Schadendorf D (2012) Dabrafenib in patients with Val600Glu or Val600Lys BRAF-mutant melanoma metastatic to the brain (BREAK-MB): a multicentre, open-label, phase 2 trial. *Lancet Oncol*.

Margolin K, Ernstoff MS, Hamid O, Lawrence D, McDermott D, Puzanov I, Wolchok JD, Clark JI, Sznol M, Logan TF, Richards J, Michener T, Balogh A, Heller KN and Hodi FS (2012) Ipilimumab in patients with melanoma and brain metastases: an open-label, phase 2 trial. *Lancet Oncol* **13**:459-465.

McCubrey JA, Milella M, Tafuri A, Martelli AM, Lunghi P, Bonati A, Cervello M, Lee JT and Steelman LS (2008) Targeting the Raf/MEK/ERK pathway with small-molecule inhibitors. *Curr Opin Investig Drugs* **9**:614-630.

Mittapalli RK, Vaidhyanathan S, Sane R and Elmquist WF (2012) Impact of P-glycoprotein (ABCB1) and breast cancer resistance protein (ABCG2) on the brain distribution of a novel BRAF inhibitor: vemurafenib (PLX4032). *J Pharmacol Exp Ther* **342**:33-40.

Nazarian R, Shi H, Wang Q, Kong X, Koya RC, Lee H, Chen Z, Lee MK, Attar N, Sazegar H, Chodon T, Nelson SF, McArthur G, Sosman JA, Ribas A and Lo RS (2010) Melanomas acquire resistance to B-RAF(V600E) inhibition by RTK or N-RAS upregulation. *Nature* **468**:973-977.

Nedelman JR, Gibiansky E and Lau DT (1995) Applying Bailer's method for AUC confidence intervals to sparse sampling. *Pharm Res* **12**:124-128.

Polli JW, Olson KL, Chism JP, John-Williams LS, Yeager RL, Woodard SM, Otto V, Castellino S and Demby VE (2009) An unexpected synergist role of P-glycoprotein and breast cancer resistance protein on the central nervous system penetration of the tyrosine kinase inhibitor lapatinib (N-{3-chloro-4-[(3-fluorobenzyl)oxy]phenyl}-6-[5-({[2-(methylsulfonyl)ethyl]amino }methyl)-2-furyl]-4-quinazolinamine; GW572016). *Drug Metab Dispos* **37**:439-442.

Rochet NM, Dronca RS, Kottschade LA, Chavan RN, Gorman B, Gilbertson JR and Markovic SN (2012) Melanoma brain metastases and vemurafenib: need for further investigation. *Mayo Clin Proc* **87**:976-981.

Schinkel AH and Jonker JW (2003) Mammalian drug efflux transporters of the ATP binding cassette (ABC) family: an overview. *Adv Drug Deliv Rev* **55**:3-29.

Siegel R, Ward E, Brawley O and Jemal A (2011) Cancer statistics, 2011: the impact of eliminating socioeconomic and racial disparities on premature cancer deaths. *CA Cancer J Clin* **61**:212-236.

Skibber JM, Soong SJ, Austin L, Balch CM and Sawaya RE (1996) Cranial irradiation after surgical excision of brain metastases in melanoma patients. *Ann Surg Oncol* **3**:118-123.

Sosman JA, Kim KB, Schuchter L, Gonzalez R, Pavlick AC, Weber JS, McArthur GA, Hutson TE, Moschos SJ, Flaherty KT, Hersey P, Kefford R, Lawrence D, Puzanov I, Lewis KD,

Amaravadi RK, Chmielowski B, Lawrence HJ, Shyr Y, Ye F, Li J, Nolop KB, Lee RJ, Joe AK and Ribas A (2012) Survival in BRAF V600-mutant advanced melanoma treated with vemurafenib. *N Engl J Med* **366**:707-714.

Laquerre S, Arnone M, Moss K, Yang J, Fisher K, Kane-Carson LS, Smitheman K, Ward J, Heidrich B, Rheault T, Adjabeng G, Hornberger K, Stellwagen J, Waterson A, Han C, Mook RA, Uehling D and King AJ (2009) A selective Raf kinase inhibitor induces cell death and tumor regression of human cancer cell lines encoding B-RafV600E mutation *Mol Cancer Ther* **8** (12 Supple): B88.

Tsao H, Atkins MB and Sober AJ (2004) Management of cutaneous melanoma. *N Engl J Med* **351**:998-1012.

Villanueva J, Vultur A, Lee JT, Somasundaram R, Fukunaga-Kalabis M, Cipolla AK, Wubbenhorst B, Xu X, Gimotty PA, Kee D, Santiago-Walker AE, Letrero R, D'Andrea K, Pushparajan A, Hayden JE, Brown KD, Laquerre S, McArthur GA, Sosman JA, Nathanson KL and Herlyn M (2010) Acquired resistance to BRAF inhibitors mediated by a RAF kinase switch in melanoma can be overcome by cotargeting MEK and IGF-1R/PI3K. *Cancer Cell* **18**:683-695.

Footnotes:

This work was supported in part by the National Institutes of Health - National Cancer Institute [Grant CA138437]

Legends for figures:

Figure 1: Chemical structure of dabrafenib (GSK2118436A)

Figure 2: *In vitro c*ellular accumulation of dabrafenib: Panel **A** shows the accumulation of prazosin (prototypical Bcrp probe substrate; positive control), and dabrafenib in MDCKII-wild-type and Bcrp1-transfected cell lines with and without Bcrp inhibitor Ko143 (0.2 µM). The accumulation of dabrafenib and vinblastine (probe substrate for P-gp) in MDR1 cells with and without P-gp inhibitor LY335979 (1 µM) is shown in Panel **B**. Data represent mean ± SD; n = 6 for all data points. ***, $p < 0.001$ compared to respective wild-type control. #, $p< 0.001$ compared to untreated transfected cell line.

Figure 3: Competition assays using prototypical probe substrate molecules: Intracellular accumulation of [^{3}H]-prazosin (Bcrp probe substrate), [^{3}H]-vinblastine (P-gp probe substrate) in Bcrp1-transfected (Panel **A**) and MDR1-transfected (Panel **B**) cell lines with increasing concentrations of dabrafenib from 0.1 µM to 50 µM. Ko: Bcrp inhibitor Ko143; LY: P-gp inhibitor LY335979. Data represent mean ± SD; n = 3 for all data points. **, $p =0.0439$ compared to untreated wild type cells. **, $p =0.003$ compared to untreated MDR1 cells.

Figure 4: Brain and plasma concentration vs time profiles of dabrafenib: Brain and plasma concentrations of dabrafenib after an i.v. dose of 2.5 mg/kg in FVB wild-type mice at 5, 15, 30, 60, and 120 minutes post dose. Brain concentrations of dabrafenib are significantly lower than plasma concentrations at all measured time points. Data represent mean ± SD, n = 3-4. *, **, ***, represent $p< 0.05$, $p< 0.001$, $p<0.0001$, respectively.

Figure 5: Brain distribution of dabrafenib in FVB wild-type and *Mdr1a/b$^{-/-}$Bcrp1$^{-/-}$* mice: Plasma concentration vs time (**A**), brain concentration vs time (**B**), and brain-to-plasma

JPET Fast Forward. Published on December 17, 2012 as DOI: 10.1124/jpet.112.201475
This article has not been copyedited and formatted. The final version may differ from this version.

concentration ratios (**C**) of dabrafenib in wild-type and *Mdr1a/b*$^{-/-}$*Bcrp1*$^{-/-}$ mice after an iv dose of 2.5 mg/kg. Plasma and brain concentrations were determined using LCMS/MS at 5, 15, 30, 60, and 120 minutes postdose of dabrafenib. Data represent mean ± SD, n = 3-4. *, **, ***, represent $p< 0.05$, $p< 0.001$, $p<0.0001$, respectively.

Figure 6: Brain distribution of dabrafenib in FVB wild-type and *Mdr1a/b*$^{-/-}$*Bcrp1*$^{-/-}$ mice after an oral dose: Plasma (**A**), brain (**B**) concentration vs time profiles, and brain-to-plasma concentration ratios (**C**) of dabrafenib in wild-type and *Mdr1a/b*$^{-/-}$*Bcrp1*$^{-/-}$ mice after an oral dose of 25 mg/kg. Plasma and brain concentrations were determined using LCMS/MS at 15, 30, 60, 120, and 240 minutes postdose of dabrafenib. Data represent mean ± SD, n = 3-4. *, **, ***, represent $p< 0.05$, $p< 0.001$, $p<0.0001$, respectively.

Figure 7: Comparison of the brain distribution of dabrafenib and vemurafenib: Plasma (**A**), brain (**B**), and brain to plasma concentration ratios (**C**) of dabrafenib and vemurafenib in wild-type and *Mdr1a/b*$^{-/-}$*Bcrp1*$^{-/-}$ mice after 1 hr postdose in separate animals (25 mg/kg, oral dose). Vemurafenib data is from our previously published results (Mittapalli et al., 2012). Data represent mean ± SD, n = 3-4. A *, **, ***, represent $p< 0.05$, $p< 0.001$, $p<0.0001$, respectively.

JPET Fast Forward. Published on December 17, 2012 as DOI: 10.1124/jpet.112.201475
This article has not been copyedited and formatted. The final version may differ from this version.

Table 1: Directional flux of dabrafenib in MDCKII-WT and MDCKII-Bcrp1 transfected cell lines:

Cell line	P_{app} (cm/s x10^{-6})		ER	CFR
	A-to-B	B-to-A		
MDCKII-WT	11.5 ± 1.4	14.1 ± 1.4	1.2	-
MDCKII-WT + 0.2 μM Ko143	16.4 ± 0.9	15.3 ± 2.6	0.9	
MDCKII-Bcrp1	1.3 ± 0.3*	27.3 ± 4.1*	21.0	17.5
MDCKII-Bcrp1 + 0.2 μM Ko143	13.2 ± 2.1#	9.6 ± 0.33#	0.7	

Note:
ER-Efflux ratio
CFR: Corrected efflux ratio
Papp: apparent permeability of dabrafenib
*significantly different compared to respective wild-type control cells
significantly different compared to untreated Bcrp1 control cells
Data represent mean ± SD; n = 3

Table 2: Directional flux of dabrafenib in MDCKII-WT and MDCKII-MDR1 Cells:

Cell line	P_{app} (cm/s x10^{-6})		ER	CFR
	A-to-B	B-to-A		
MDCKII-WT	2.6 ± 1.0	7.7 ± 1.6	3.0	-
MDCKII-WT + 1 µM LY335979	5.5 ± 0.4	5.2 ± 0.7	0.90	
MDCKII-MDR1	0.7 ± 0.3*	7.9 ± 1.9	11.4	3.8
MDCKII-MDR1 + 1 µM LY335979	4.9 ± 0.52#	5.2 ± 1.4	1.1	

Note:
ER-Efflux ratio
CFR: Corrected efflux ratio
Papp: apparent permeability of dabrafenib
*significantly different compared to respective wild-type control cells
significantly different compared to untreated MDR1 control cells
Data represent mean ± SD; n = 3

JPET Fast Forward. Published on December 17, 2012 as DOI: 10.1124/jpet.112.201475
This article has not been copyedited and formatted. The final version may differ from this version.

Table 3:

Comparison of Pharmacokinetic Parameters of Dabrafenib in FVB Wild-type and *Mdr1a/b$^{-/-}$Bcrp1$^{-/-}$* Mice After an i.v. dose of 2.5 mg/kg

	Wild-type		*Mdr1a/b$^{-/-}$Bcrp1$^{-/-}$* Mice	
	Plasma	**Brain**	**Plasma**	**Brain**
Terminal rate Constant (min^{-1})	0.03	0.036	0.024	0.026
Half-life (min)	23.7	19.1	28.3	26.6
Clearance (mL/min/kg)	24.2		28.4	
Volume of Distribution (L/kg)	0.83		1.2	
$AUC_{0 \rightarrow t\ last}$ (µg · min /mL)[1]	120.9 ± 15.8	2.8 ± 0.4	101.4 ± 8.7	42.1 ± 3.4*
K_p[2]	0.023		0.42	
K_p Ratio[3]	18.3			

1. Area under the curve from time zero to 2 hour post dose
2. Kp = AUC_{brain}/AUC_{plasma}
3. Kp Ratio = (Kp in *Mdr1a/b$^{-/-}$Bcrp1$^{-/-}$* mice) / (Kp in wild-type mice)
4. *, $p < 0.05$ compared to wild-type AUC_{brain}

JPET Fast Forward. Published on December 17, 2012 as DOI: 10.1124/jpet.112.201475
This article has not been copyedited and formatted. The final version may differ from this version.

Table 4:

Pharmacokinetic metrics in FVB wild-type and *Mdr1a/b*$^{-/-}$*Bcrp1*$^{-/-}$ Mice after Oral Dosing with 25 mg/kg Dabrafenib (Data presented as Mean ± SEE)

Mouse Genotype	Tissue	C_{max} (µg/mL)	AUC_{last}[1] (µg.min/mL)	Kp[2]	Kp Ratio[3]
Wild-type	Plasma	0.143 ± 0.014	15.8 ± 3.0	0.044	5.7
Wild-type	Brain	0.007 ± 0.001	0.69 ± 0.22		
***Mdr1a/b*$^{-/-}$*Bcrp1*$^{-/-}$**	Plasma	0.324 ± 0.085	31.1 ± 5.1[#]	0.25	
***Mdr1a/b*$^{-/-}$*Bcrp1*$^{-/-}$**	Brain	0.098 ± 0.022	7.6 ± 1.3*		

1. Area under the curve from time zero to 4 hour post dose
2. Kp = AUC_{brain}/AUC_{plasma}
3. Kp Ratio = Kp in TKO Mice / Kp in WT Mice
4. [#], p = 0.0414 compared to WT plasma
5. *, p = 0.002 compared to WT brain

JPET Fast Forward. Published on December 17, 2012 as DOI: 10.1124/jpet.112.201475
This article has not been copyedited and formatted. The final version may differ from this version.

Table 5:

Comparison of brain distribution of vemurafenib and dabrafenib in FVB wild-type mice after an i.v. dose of 2.5 mg/kg

	Dabrafenib		Vemurafenib[#]	
	Plasma	**Brain**	**Plasma**	**Brain**
Terminal rate Constant (min^{-1})	0.031	0.036	0.0051	0.0047
Half-life (min)	23.7	19.1	136	148
Clearance (mL/min/kg)	24.2		1.6	
Volume of Distribution (L/kg)	0.83		0.316	
$AUC_{0 \rightarrow t\ last}$ (min · µg/mL)	120.9 ± 15.8	2.8 ± 0.4	1663 ± 140	6.5 ± 0.9
K_p	0.023		0.004	

[#] From previously published data (Mittapalli et al., 2012).

Figure # 1

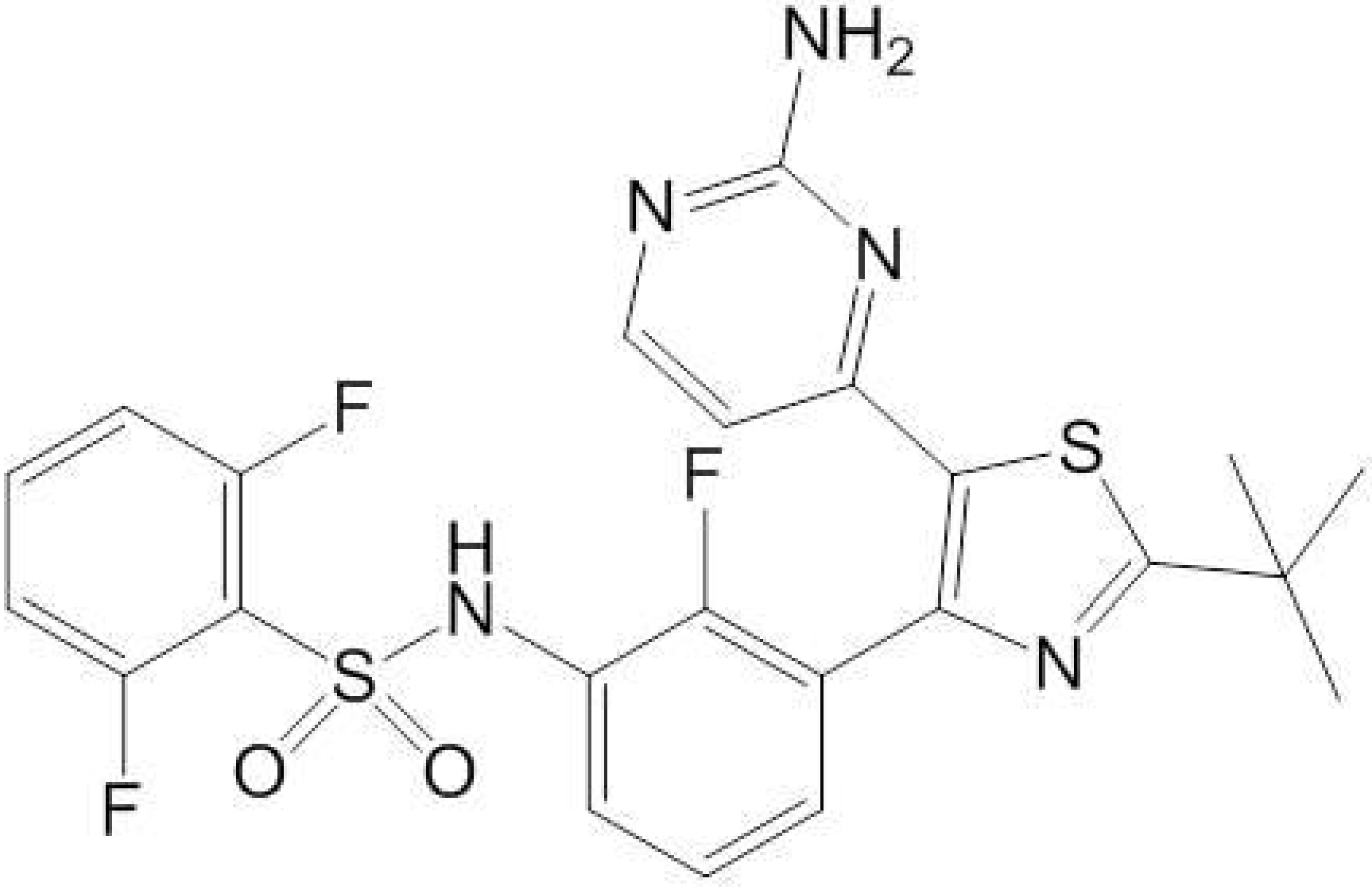

Figure # 2

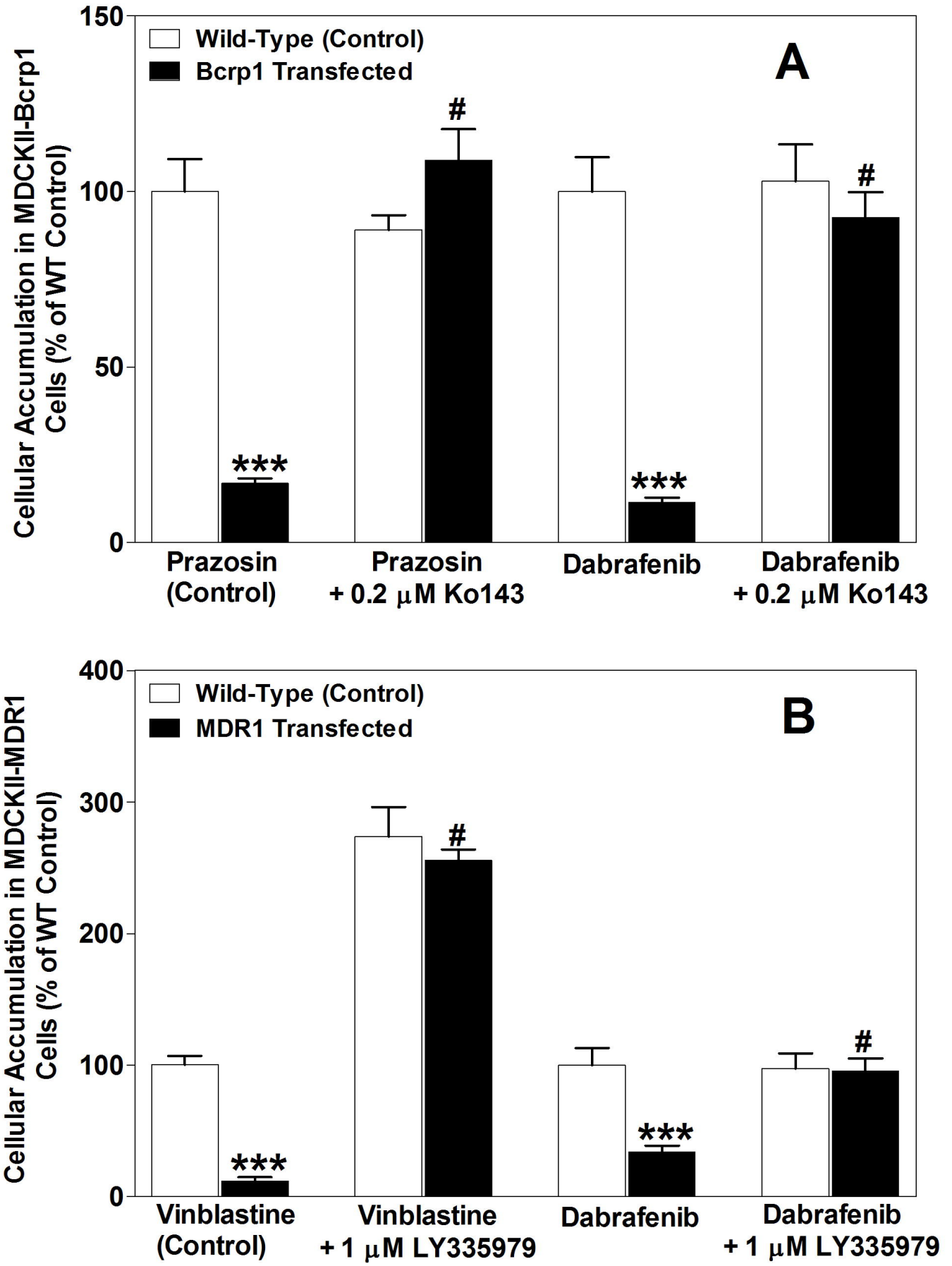
A
Wild-Type (Control)
Bcrp1 Transfected
Cellular Accumulation in MDCKII-Bcrp1 Cells (% of WT Control)
150
100
50
0
***
#
***
#
Prazosin (Control)
Prazosin + 0.2 μM Ko143
Dabrafenib
Dabrafenib + 0.2 μM Ko143
B
Wild-Type (Control)
MDR1 Transfected
Cellular Accumulation in MDCKII-MDR1 Cells (% of WT Control)
400
300
200
100
0
***
#
***
#
Vinblastine (Control)
Vinblastine + 1 μM LY335979
Dabrafenib
Dabrafenib + 1 μM LY335979

Figure # 3

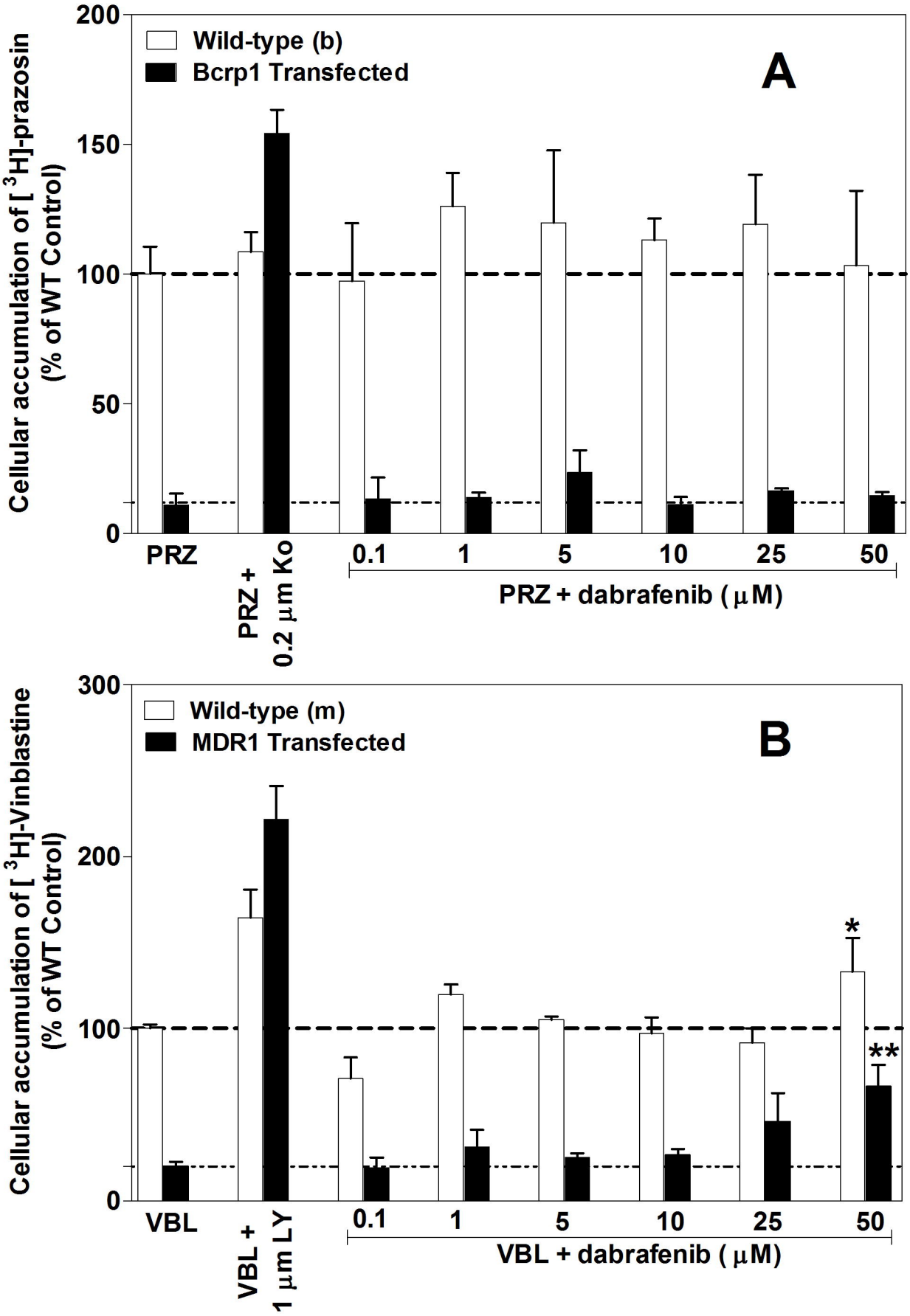
A
Wild-type (b)
Bcrp1 Transfected
Cellular accumulation of [3H]-prazosin (% of WT Control)
200
150
100
50
0
PRZ
PRZ + 0.2 μm Ko
0.1
1
5
10
25
50
PRZ + dabrafenib (μM)
B
Wild-type (m)
MDR1 Transfected
Cellular accumulation of [3H]-Vinblastine (% of WT Control)
300
200
100
0
VBL
VBL + 1 μm LY
0.1
1
5
10
25
50
VBL + dabrafenib (μM)
*
**

Figure # 4

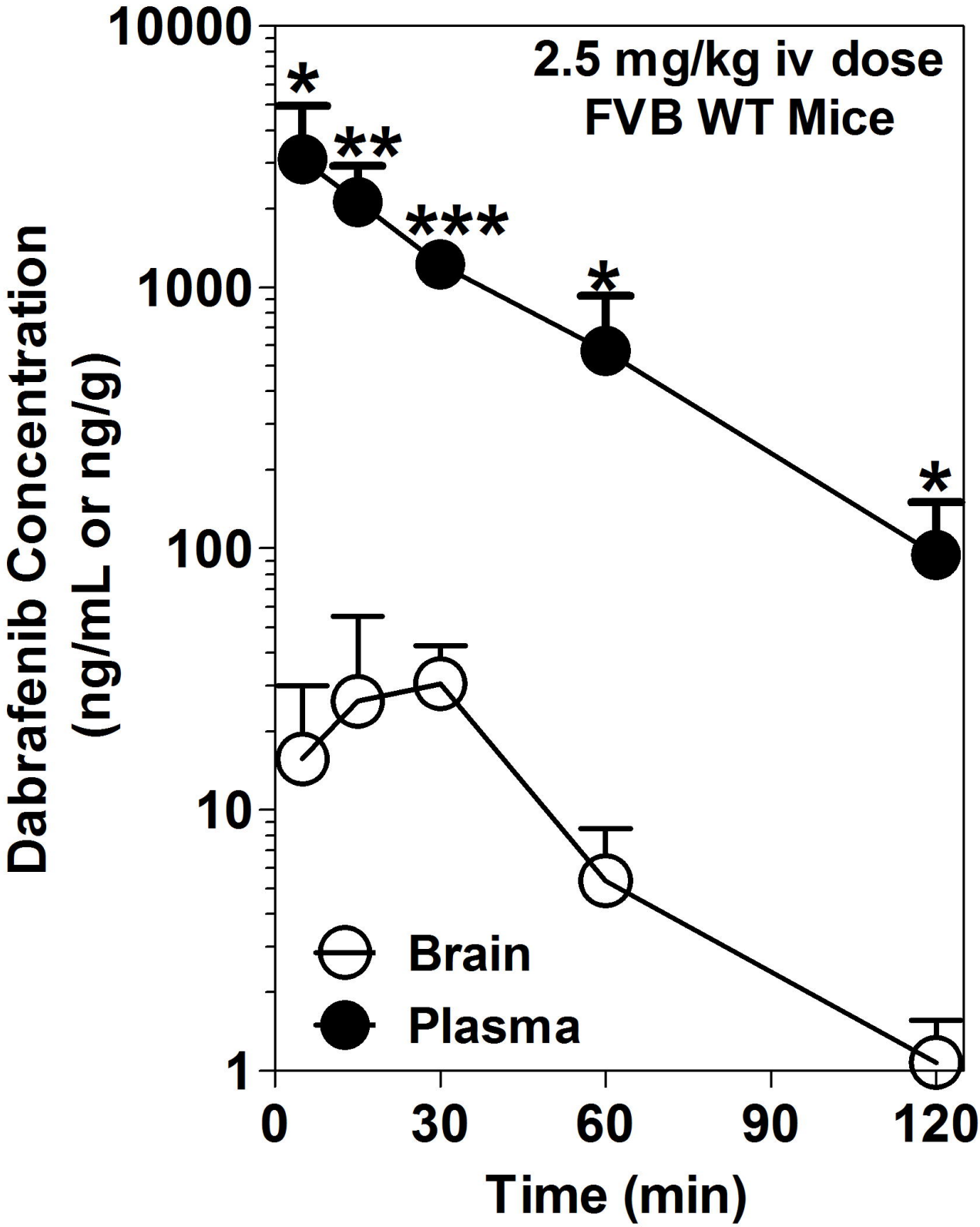
2.5 mg/kg iv dose
FVB WT Mice
Dabrafenib Concentration
(ng/mL or ng/g)
10000
1000
100
10
1
*
**
***
*
*
Brain
Plasma
0
30
60
90
120
Time (min)

Figure # 5

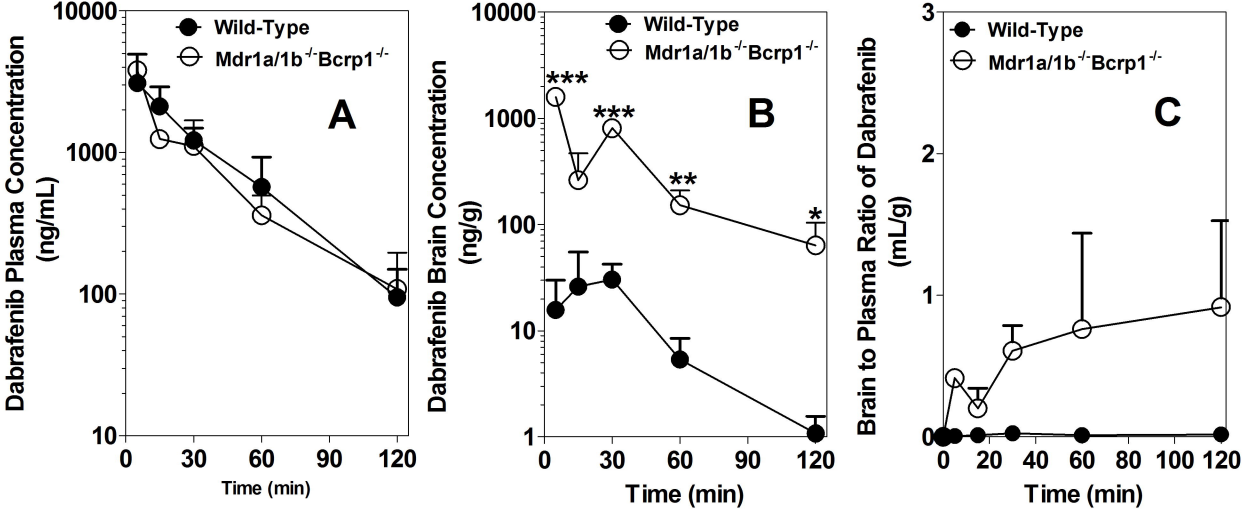
A
Wild-Type
Mdr1a/1b-/-Bcrp1-/-
Dabrafenib Plasma Concentration (ng/mL)
10000
1000
100
10
0
30
60
90
120
Time (min)
B
Wild-Type
Mdr1a/1b-/-Bcrp1-/-
Dabrafenib Brain Concentration (ng/g)
***
***
**
*
10000
1000
100
10
1
0
30
60
90
120
Time (min)
C
Wild-Type
Mdr1a/1b-/-Bcrp1-/-
Brain to Plasma Ratio of Dabrafenib (mL/g)
3
2
1
0
0
20
40
60
80
100
120
Time (min)

Figure # 6

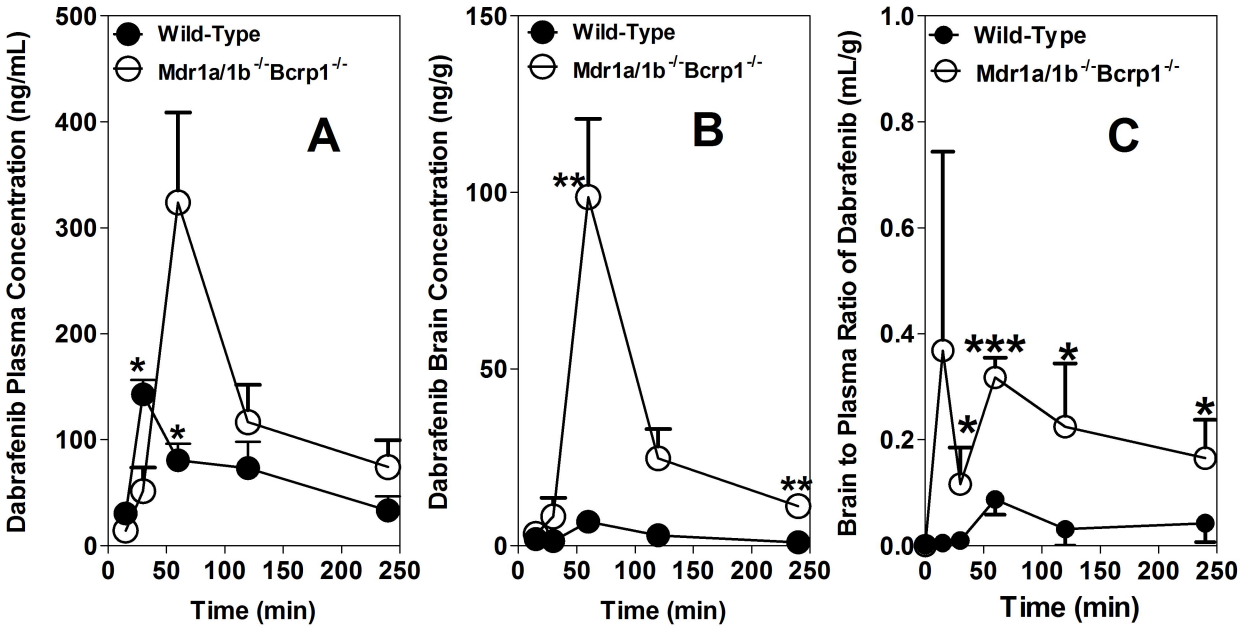
Wild-Type
Mdr1a/1b-/-Bcrp1-/-
A
Dabrafenib Plasma Concentration (ng/mL)
Time (min)
B
Dabrafenib Brain Concentration (ng/g)
Time (min)
C
Brain to Plasma Ratio of Dabrafenib (mL/g)
Time (min)

Figure # 7

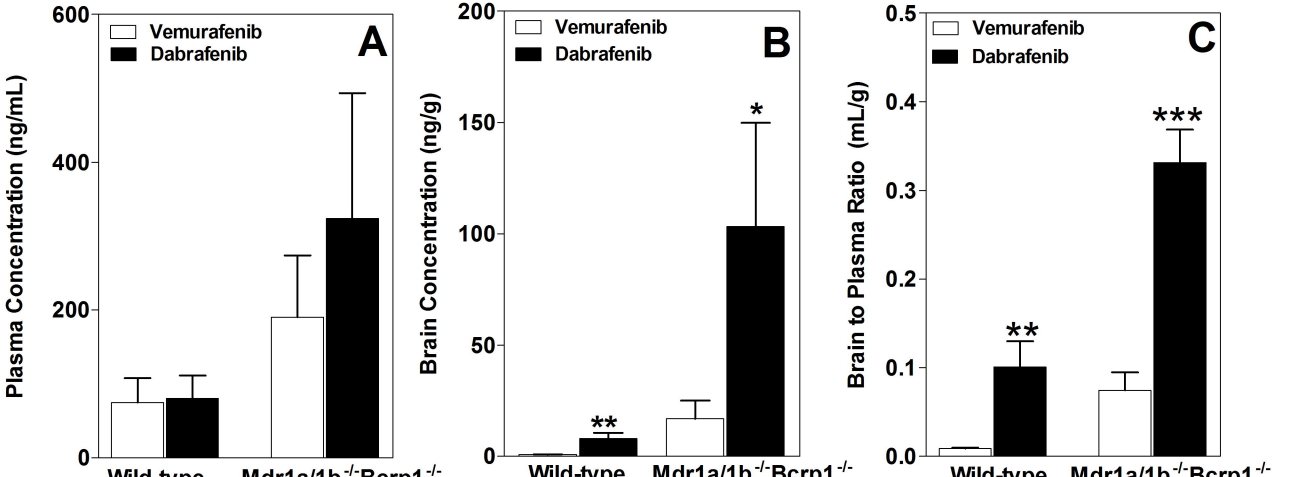
A
Vemurafenib
Dabrafenib
Plasma Concentration (ng/mL)
600
400
200
0
Wild-type
Mdr1a/1b-/-Bcrp1-/-
B
Vemurafenib
Dabrafenib
Brain Concentration (ng/g)
200
150
100
50
0
*
**
Wild-type
Mdr1a/1b-/-Bcrp1-/-
C
Vemurafenib
Dabrafenib
Brain to Plasma Ratio (mL/g)
0.5
0.4
0.3
0.2
0.1
0.0
**
***
Wild-type
Mdr1a/1b-/-Bcrp1-/-

Mechanisms Limiting Distribution of the BRAF^{V600E} Inhibitor Dabrafenib to the Brain: Implications for the Treatment of Melanoma Brain Metastases

Rajendar K Mittapalli, Shruthi Vaidhyanathan, Arkadiusz Z. Dudek, and William F. Elmquist

Journal of Pharmacology and Experimental Therapeutics

Supplemental Figure 1:

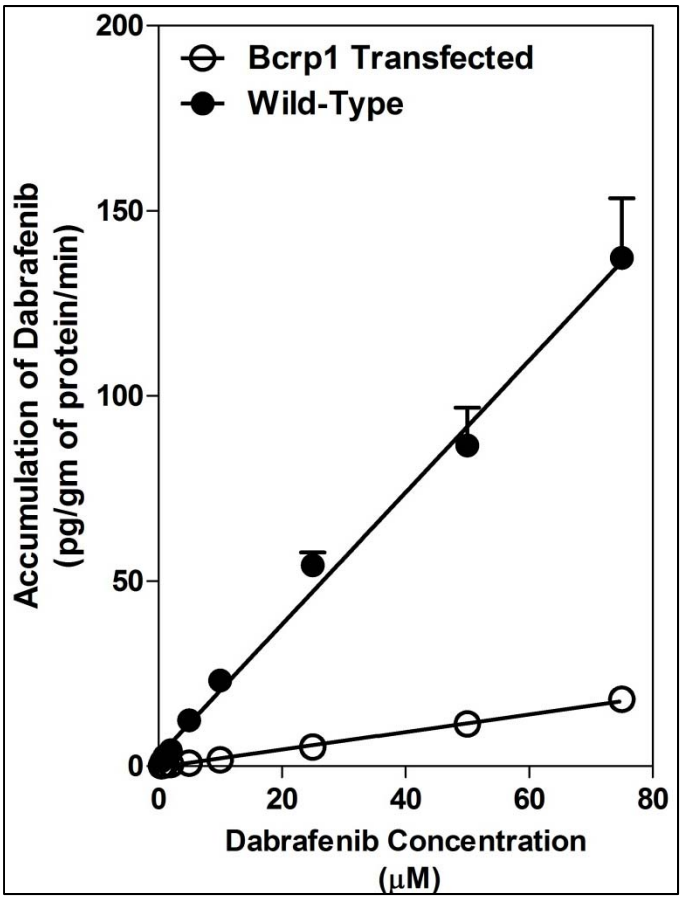

Figure Legend: Accumulation of different concentrations (0.5 to 75 μM) of dabrafenib in MDCKII- wild type and Bcrp1 transfected cell lines. The data show a linear correlation between concentration and cellular accumulation indicating no saturation of these active efflux transporters. Data represent Mean ± SD; n= 3 for all data sets.

Mechanisms Limiting Distribution of the BRAF^{V600E} Inhibitor Dabrafenib to the Brain: Implications for the Treatment of Melanoma Brain Metastases

Rajendar K Mittapalli, Shruthi Vaidhyanathan, Arkadiusz Z. Dudek, and William F. Elmquist

Journal of Pharmacology and Experimental Therapeutics

Supplemental Figure 2:

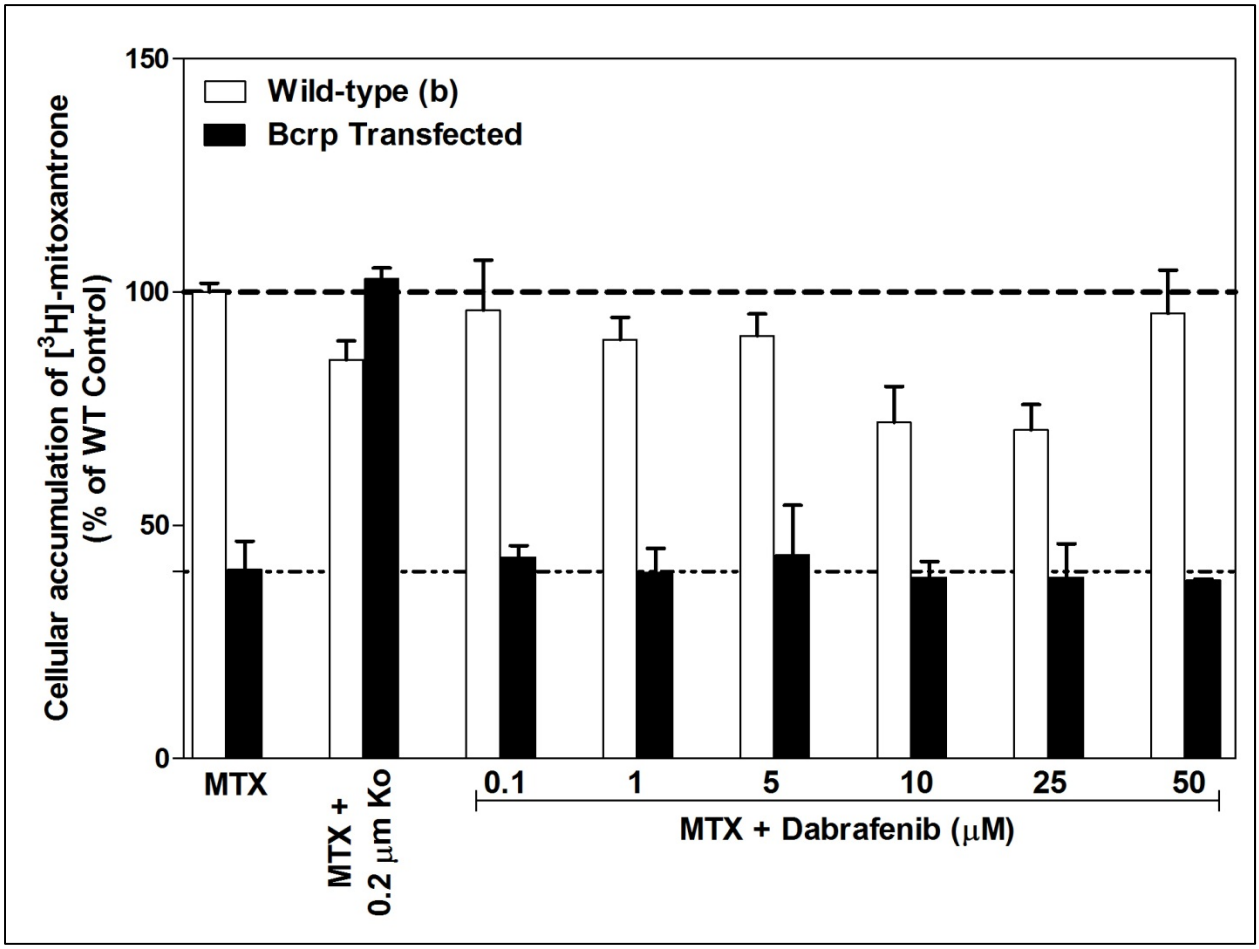

Figure Legend: Intracellular accumulation of [^{3}H]-mitoxantrone (MTX; Bcrp probe substrate) in Bcrp1-transfected cell lines with increasing concentrations of dabrafenib from 0.1 µM to 50 µM. Ko: Bcrp inhibitor Ko143; Data represent mean ± SD; n = 3 for all data points.

Mechanisms Limiting Distribution of the BRAF^{V600E} Inhibitor Dabrafenib to the Brain: Implications for the Treatment of Melanoma Brain Metastases

Rajendar K Mittapalli, Shruthi Vaidhyanathan, Arkadiusz Z. Dudek, and William F. Elmquist

Journal of Pharmacology and Experimental Therapeutics

Supplemental Figure 3:

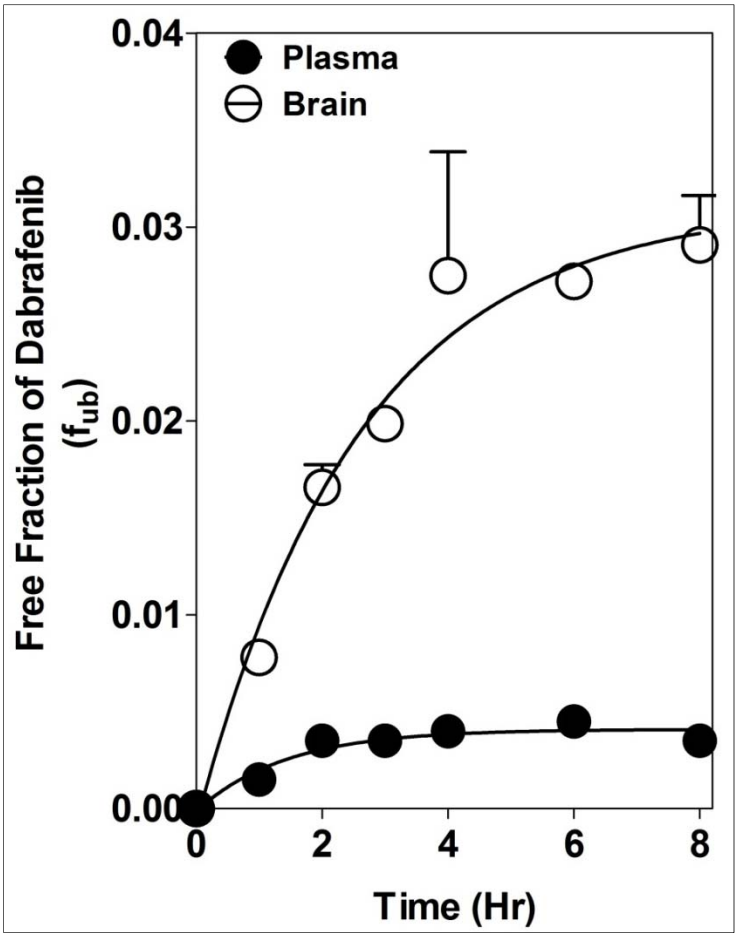

Figure Legend: Equilibrium dialysis in plasma and brain homogenate: The graph shows the free fraction of dabrafenib (fraction unbound, f_{ub}) in plasma and brain homogenate with respect to time. The data indicate that equilibrium is achieved in ~6hrs in both plasma and brain homogenate.